Journal of Chemistry and Chemical Sciences, *Vol.11(12),150-157, December, 2021* *ISSN 2229-760X (Print)*
(An International Research Journal), *www.chemistry-journal.org* *ISSN 2319-7625 (Online)*

Synthesis of Ag/ZnO Nanoparticles by a Pyrolytic Method: Characterization and Photocatalytic Activity Study

Tanmay Chattopadhyay*

*Department of Chemistry,
Diamond Harbour Women's University,
Diamond Harbour Road, Sarisha, South 24 Pgs, 743368, INDIA.
email: tanmayc2003@gmail.com,

(Received on: December 2, 2021)

ABSTRACT

Ag/ZnO nanoparticles have been prepared via simple thermal treatment of a hetero tri-nuclear precursor compound $[Zn(Imdz)_4(Ag(CN)_2)_2]$ (1) (Imdz = Imidazole) as precursors at 550 °C in air for 4 h. A variety of techniques such as UV-Vis spectroscopy, IR spectroscopy, XRPD, XPS, SEM, TEM and EDX were used for their characterization. These nanoparticles show optical band gap at 2.75 eV. Photocatalytic reactivity of these nanoparticles has been evaluated by studying the degradation of C. I. Reactive Yellow 84 (RY 84), a popular and widely used reactive dye in cotton industry.

Keywords: Pyrolytic technique, Ag/ZnO nanoparticles, Semiconductors, Photocatalytic reactivity, C. I. Reactive Yellow 84.

INTRODUCTION

Organic dye pollutants, a dreadful hazard typically comes from the industrial waste water, such as textile, leather goods, cosmetics, food, plastics, consumer electronics; etc[1-3]. They generally reveal a distinct toxic effect to marine plants and species and therefore become an immense threat our whole living hood. So, to avoid these hazardous effect these industry wastes have to be treated earlier before discharging them into the environment. So it has become a challenge to the chemists to degrade these dyes as to avoid the enormous toxic effect. However, degradation through chemical reactions may involve liberation of harmful chemicals as well as gases into the environment, due to such limitations, it is the high time for proper, robust and green non-toxic materials plus processes which have to be designed

and practiced to handle the issue of this environmental pollution. Now, Nanotechnology, the latest branch of modern science, has played a crucial function in recent time to handle such issues in more effective manners. Nowadays, metal oxide nanoparticles have been employed frequently for degradation of organic dyes. Advancement in photo catalytic research led to use of oxygen rich metal oxides nano-particles for help of the oxidation of organic molecules facilitating green decomposition[4,5]. ZnO has got more attention due to its stronger luminescent properties, broader ultraviolet (UV) light absorption, and more economic than TiO_2. The doped ZnO nanostructures have attracted considerable focus for its photocatalytic applications[6,7], where the effect of doping significantly enhance the luminescent properties of this material, as well as the photocatalytic degradation activity[8-10]. In addition to this, it has been establish from literature that the photocatalytic degradation activity of ZnO is improved by silver addition, which has been attributed to the doping induced modification of surface properties[11]. Although, the oxidation states, structural and optical properties of Ag incorporated ZnO nanoparticles have not been extensively studied. There are several methods[12] reported in literature to synthesize nano-structures of Ag doped ZnO[13-15], like electrochemical[16], photochemical[17], sol–gel[18], hydrothermal[19], microwave[20], and flame spray pyrolysis[21]. But although those above listed methods require high synthesis temperature or difficult synthesis conditions and sophisticated equipments. With those lack of findings therefore motivated us towards our present work where, Ag/ZnO nanoparticles have been successfully synthesized by us with simple pyrolytic technique, without using any costly equipment. These nanostructures are further characterized by XPS, XRPD, SEM and TEM and successfully employed as a simple but effective dye degraded agent. All these synthesis, characterisation and photocatalytic degradation properties of our doped nanoparticles have been effectively portrayed in this manuscript.

EXPERIMENTAL

Materials and Methods

All chemicals were obtained from commercial sources and used as received. Solvents were dried according to standard procedure and distilled prior to use. Water used in all physical measurement and experiments was Milli-Q grade. Imidazole, zinc perchlorate hexahydrate and potassium dicyanoargentate (I) were purchased from Sigma-Aldrich (Kolkata, India). C. I. Reactive Yellow 84 was purchased from Atul India Ltd. All other chemicals were of AR grade. Infrared spectra (4000–500 cm^{-1}) were obtained at 27 °C using a Perkin–Elmer RXI FT-IR spectrometer with KBr pellets. X-ray powder diffraction patterns of the products were recorded on a Philips (PANalytical), (model: PW1830) X-ray diffractometer equipped with graphite monochromatized Cu-Ka radiation. Scanning electron microscope (SEM) images were taken with JEOL JSM-6700F field emission microscope. Electronic spectra (800–200 nm) were obtained at 27 °C using a Shimadzu UV-3101PC. Transmission electron microscopy (TEM) images were collected with a JEOL (Japan) JEM 2100 high-resolution transmission electron microscope operating at 200 kV. XPS

measurements were performed at room temperature with a SPECS EA10P hemispherical analyzer using both non-monochromatic Mg Ka (1253.6 eV) and Al Ka (1486.6 eV) radiation (300 W) as excitation source in a base pressure of ~ 10^{-9} mbar.

Syntheses of the complex and the catalyst

A methanolic solution (5 mL) of zinc perchlorate hexahydrate (0.37 g, 1 mmol) was added in a drop wise manner to a methanolic solution (10 mL) of imidazole (0.272 g, 4 mmol) and the resulting solution was then stirred at room temperature for half an hour. Methanolic solution (5 mL) of potassium dicyanoargentate (I) (0.398 g, 2 mmol) was then added to it and the resulting solution was stirred at room temperature for another 1 h. The resulting solution was then filtered and kept in dark in a $CaCl_2$ dessicator. After few days product precipitated out, this was further recrystalised from ethanol for further purification of the compound.

For the preparation of large amounts of Ag/ZnO nanoparticles from the complexes, about 5 g of the complex was heated at 550 °C for 4 h in big platinum crucibles separately in a muffle furnace. The obtained Ag/ZnO nanoparticles were then washed with methanol followed by water repeatedly to remove the impurity. The pure nanoparticles obtained were characterized by FT-IR spectroscopy, XRPD, XPS, Solid UV–Visible spectroscopy, SEM and TEM images.

All the photocatalytic experiments were carried out in a 100 mL capacity borosil glass reactor under similar conditions with exposure of light. First, a calibration curve of the dye was plotted so that the concentration of the dye in any unknown sample was estimated by measuring the absorbance intensity by a same method as reported earlier[22] . A series of dye solutions in water were prepared of fixed concentration (40 mg/L), and 10 mg of Ag/ZnO nanoparticles were dispersed in 50 mL of these solutions and exposed to light. At different time intervals, definite aliquots were taken out with the help of a syringe and filtered through a Millipore syringe filter. The absorption spectra were recorded on UV-vis spectrophotometer and rate of decolorization was observed in terms of change in intensity at λ_{max}, i.e., 410 nm for dye. The experiment was performed for 5 h and within this time the dye was completely degraded.

RESULTS AND DISCUSSION

The FTIR spectra of synthesized Ag/ZnO nanoparticles were recorded in the range from 400 to 4000 cm^{-1} at room temperature (Fig. 1). The FTIR spectrum of the Ag/ZnO nanocomposite material contains several bands with remarkable features. The bands between 400 and 750 cm^{-1} can be correlated to metal oxide bond (ZnO)[23-25]. Bands around 900-1500 cm^{-1} are due to the oxygen stretching and bending frequency[26,27]. The spectral band at 502 cm^{-1} and the band at 700-800 cm^{-1} clearly show the presence of ZnO and Ag ions approximately equal with the reported literature[28]. On doping, stronger and wider absorption, bands observed in the region ~ 700-800 cm^{-1} due to the organic capping of silver[29]. It is

evident from the FTIR data that the Zn-O vibrational mode more significantly observed and this clearly concludes a strong doping between Ag and ZnO[30].

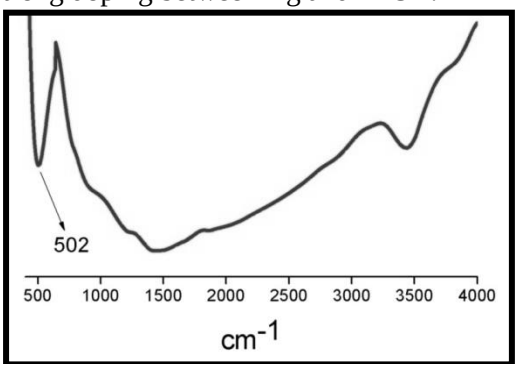

Figure 1. FT-IR spectrum of synthesized Ag/ZnO nanoparticles.

XRPD pattern of the Ag/ZnO is shown in Fig. 2. XRPD patterns of undoped ZnO exhibited the characteristic peaks of hexagonal structure. XRPD pattern of the sample reveals only the diffraction peaks attributable to Ag and ZnO nanoparticles. The peaks at 2θ = 39.2°, 44.5°, 64.7°, 79.1° and 81.5°, which can be perfectly related to (111), (200), (220), (311), and (222) crystal planes of face centered cubic (fcc) silver, respectively[31]. Other peaks at 2θ = 32.1°, 34.9°, 36.8°, 47.2°, 56.9°, 62.2°, 68.4° and 69.1° are corresponds to (100), (002), (101), (102), (110), (103), (112) and (201) planes of monoclinic ZnO as reported previously[32].

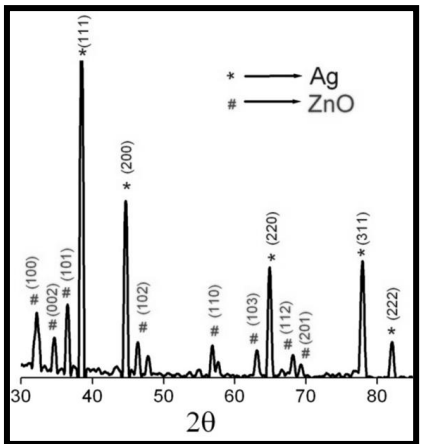

Figure 2. XRPD spectrum of synthesized Ag/ZnO nanoparticles.

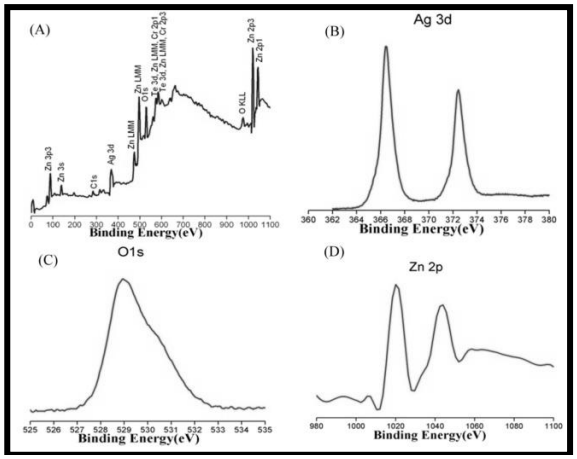

Figure 3. (A) XPS full spectrum of synthesized Ag/ZnO nanoparticles; (B) Ag 3d spectrum; (C) O 1s spectrum and (D) Zn 2p spectrum.

The XPS spectra of Ag/ZnO are shown in Fig. 3A. The full-scan spectrum in Fig. 3 allows the identification of Zn, O, C and Ag, confirming the presence of these elements in

the sample. The carbon (C1s) peak at 284.8 eV comes from the adsorption of organic contaminants on the surface of the sample during handling. Figs. 3B, 3C and 3D show the high-resolution XPS spectra of Ag (3d), O (1S) and Zn (2P) respectively. According to Fig. 3D, the Zn (2p) consists of two peaks positioned at 1022.3 and 1044.7 eV for Zn (2p), in concurrence with the formerly reported binding energies (BE) of ZnO[33,34]. For pure ZnO nanoparticles, these peaks are located at 1021.4 and 1044.5 eV, respectively. The location of these peaks slightly shifts to higher BE values due to the Ag-doping content. Fig. 3B consists of two peaks positioned at 367.3 and 373.1eV for Ag (3d). Fig. 3C the O 1s spectrum has a major peak at 529.7 eV.

SEM image of nanoparticles generated from Ag/ZnO is represented in Fig. 4 (A).The particles are well aggregated. Some of the particles are hexagonal where rests are spherical in nature as shown in the image. Spherical particles are attached on the surface of hexagonal particles. To identify the particles and to determine the exact size transmission electron microscopic (TEM) image of the particles was taken. The transmission electron microscopy image of the nanoparticles show nearly spherical shaped particles as presented in SEM image with a mean size of 20 ± 5 nm (Fig. 4 (B)). EDX spectrum clearly indicates the four elements, C, Zn, O, and Ag, are present in synthesized nanocomposite (Fig. 4C).

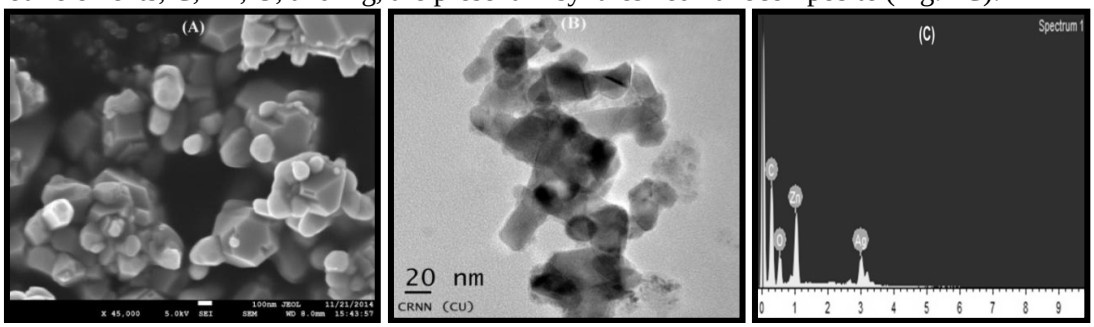

Fig.-4 (A) Scanning electron microscopy (SEM) image (B) Transmission electron microscopy (TEM) image and (C) Energy-dispersive X-ray spectroscopy (EDX) spectrum of synthesized Ag/ZnO nanoparticles.

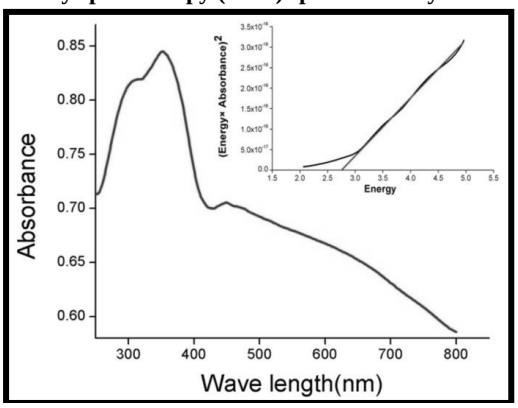

Figure 5. UV-Vis absorbance of synthesized Ag/ZnO nanoparticles. Inset picture indicates the band gap energy of the nanoparticles.

UV-Vis spectroscopy analyses were performed to determine the effect of Ag on the optical properties of the ZnO nanoparticles. The room temperature UV–visible absorption spectra of Ag/ZnO nanoparticles are shown in Fig. 5. It can be seen from Fig. 5 that there is a prominent absorption peak at 374 nm for Ag/ZnO nanoparticles. It is well known that the relationship between absorption coefficient (α) near the absorption edge and the optical band gap (*E*g) obeys the following equation for a semiconductor[35,36] $(\alpha h\nu)^n = B(h\nu - Eg)$, where B is the parameter that relates to the effective masses associated with the valence and conduction bands, *hν* is the photon energy, and n is either two for a direct transition or half for an indirect transition. From the spectra, we estimated the band gap of Ag/ZnO nanoparticles is 2.75eV (Fig. 5).For the pure ZnO nanoparticles , Eg was determined as 3.241 eV[33], which lowers to 2.75eV. Due to Ag doping decrease in the Eg value of Ag/ZnO nanoparticles[37,38].

Photocatalytic process of dye degradation

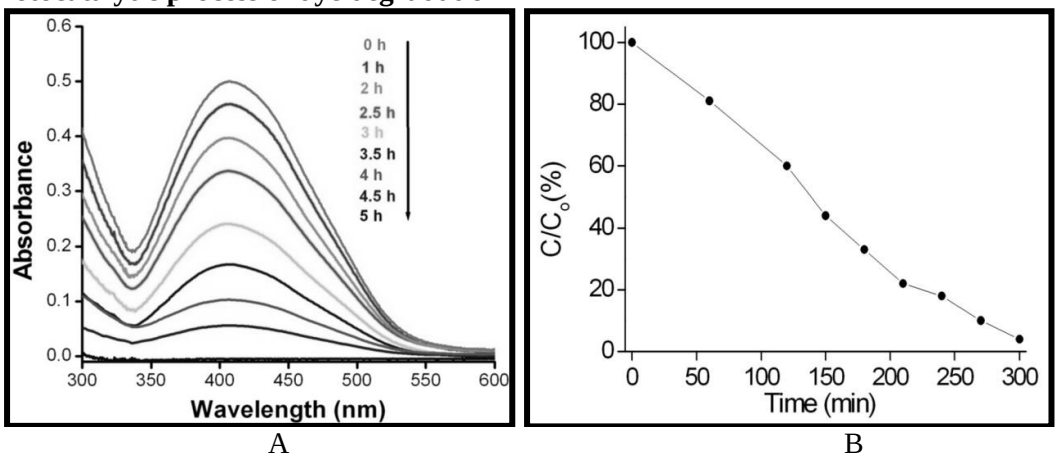

Figure 6. (A) UV–vis spectra of Ag/ZnO nanoparticles at different time interval. (B) $\ln(C_0/C)$ versus *t* plots.

In order to study the photocatalytic property of our synthesized products, we measured the optical property changes of C. I. Reactive Yellow 84 aqueous solutions in the absence as well as in the presence of Ag/ZnO nanoparticles under the exposure of light (Fig. 6) for 5 h. In presence of our photocatalysts, within 5 h ~100 % of dye was degraded (Fig. 6). Reactive Yellow 84 under UV irradiation follows pseudo-first-order kinetics with respect to C. I. Reactive Yellow 84. This relation can be described as: $\ln(C_0/C) = k_a t$, where C_0 is the concentration when UV irradiation starts, and k_a is the apparent photo-degradation rate constant[22]. The k_a values calculated from the slope of linear plot $\ln(C_0/C)$ versus *t* plots is (Fig. 6B) for this Ag/ZnO nanoparticles respectively. Generally, in the photocatalytic degradation of organic dye solutions, hydroxyl radicals are considered to play an essential role[39]. We presume that in the present case also hydroxyl radical formation is responsible for the degradation of the reactive dye used in this study.

CONCLUSION

In the present study, Ag/ZnO nanoparticles have been successfully synthesized by a simple pyrolytic technique using coordination polymer $[Zn(Imdz)_4(Ag(CN)_2)_2]$. Here silver addition effect on the structural/optical properties and photocatalytic activities of ZnO nanoparticles has been shown. The synthesized NPs were characterized successfully by XRPD, SEM, TEM, XPS, EDX and UV–vis. The XPS spectrum of Zn 2p showed that the split value of binding energy could be the characteristic value of ZnO. The UV-VIS results showed that Ag addition decreases the band gap of ZnO.

REFERENCES

1. K. Rajeshwar, M. E. Osugi , W. Chanmanee, C. R.Chenthamarakshan, M. V. B Zanoni, P. Kajitvichyanukul and R. Krishnan-Ayer, *J Photochem Photobiol C*, 9, 171 (2008).
2. M. A. Rauf and S. S. Ashraf, *Chem Eng J*, 151, 10 (2009).
3. F. Han, V. S. R. Kambala, M. Srinivasan, D. Rajarathnam and R. Naidu , *Appl Catal A*, 359, 25 (2009).
4. N. Zhang, M. Q. Yang, S. Liu, Y. Sun and Y. J. Xu, *Chem Rev*, 115, 10307 (2015).
5. A. Weir, P. Westerhoff, L. Fabricius, K. Hristovski and N. Von Goetz , *Environ Sci Technol*, 46, 2242 (2012).
6. S. T. Kochuveedu, Y. H. Jang and D. H. Kim, *Chem Soc Rev*, 42, 8467 (2013).
7. A. Di Paola, E. García-López, G. Marcí and L. Palmisano, *J Hazard Mater*, 211, 3 (2012).
8. E. Mosquera, I. del Pozo and M. Morel, *J Solid State Chem*, 206, 265 (2013).
9. K. Liu, B. F. Yang, H. Yan, Z. Fu, M. Wen, Y. Chen and J. Zuo, *Appl Surf Sci*, 255 2052 (2008).
10. H. Xue , X. L. Xu, Y. Chen, G. H. Zhan and S. Y. Ma, *Appl Surf Sci*, 255, 1806 (2008).
11. R. K. Sahu, K. Ganguly, T. Mishra, M. Mishra, R. S. Ningthoujam, S. K. Roy and L. C. Pathak, *J Colloid Interface Sci*, 366, 8 (2012).
12. X. Wen, Y. Fang, Q. Pang, C. Yang, J. Wang, W. Ge, K. S. Wong and S. Yang, *J Phys Chem B*, 109, 15303 (2005).
13. L. E. Greene, B. D. Yuhas, M. Law, D. Zitoun and P. Yang, *Inorg Chem*, 45, 7535 (2006).
14. R. Saravanan, N. Karthikeyan, V. K. Gupta, E. Thirumal, P. Thangadurai, V. Narayanan and A. Sthepen, *Mater Sci Eng C*, 33, 2235 (2013).
15. J. Xu, Y. Chang, Y. Zhang, S. Ma, Y. Qu and C. Xu, *Appl Surf Sci*, 255, 1996 (2008).
16. Y. Zheng, C. Chen, Y. Zhan, X. Lin, Q. Zheng, K. Wei, and J. Zhu, *J Phys Chem C*, 112, 10773 (2008).
17. J. Z. Wu, J. P. Tu, Y. F. Yuan, M. Ma, X. L. Wang, L. Zhang, R. L. Li, and J. Zhang, *J Alloy Compd*, 479, 624 (2009).
18. T. Alammar and A.V. Mudring, *J Mater Sci*, 44, 3218 (2009).
19. R. Georgekutty, M. K. Seery, and S. C. Pillai, *J Phys Chem C*,112, 13563 (2008).
20. Y. Zhang and J. Mu, *J Colloid Interface Sci*, 309, 478 (2007).

21. C. Karunakaran, V. Rajeswari, and P. Gomathisankar, *Solid State Sci,* 13, 923 (2011).
22. S. Mondal, T. Chattopadhyay, S. Das, S. R. Maulik, S. Neogi, and D. Das, *Ind Journal of Chem*, 51A, 807 (2012).
23. Y. J. Kwon, K. H. Kim and C. S. Lim, *J Ceram Proc Res*, 3, 146 (2002).
24. R. F. Silva and M. E. D. Zaniquelli, *Colliod Surf Physicochem Eng Aspect*, 198 551 (2002).
25. H. Li, J. Wang, and H. Liu, *Vacuum*, 77, 57 (2004).
26. S. Kurian, S. Sebastian, J. Mathew and K. C. George, *Ind J Pure & Appl Phys*, 42, 926 (2004).
27. B. S. R. Devi, R. Raveendran and A. V. Vaidyan, *Pramana*, 68, 679 (2007).
28. S. Suwanboon, *Sci. Asia*, 34, 31 (2008).
29. A. H. Shah, E. Manikandan, M. B. Ahmed and V. Ganesan, *J Nanomed Nanotechol*, 4, 2 (2013).
30. D. Sahu, B. S. Acharya and A. K. Panda, *J Ultrason Sonochem*, 18, 601 (2011) .
31. S. Kalathil, J. Lee and M. H. Cho, *Green Chem*, 13, 1482 (2011).
32. S. K. Gandomani, R. Yousefi, F. Jamali-Sheini and N. M. Huang, *Ceramic international*, (2013).
33. Ö. A. Yildirim, H.E. Unalan and C. Durucan, *J Am Ceram Soc*, 96, 766 (2013).
34. S. A. Ansari, M. M. Khan, S. Kalathil, A. Nisar, J. Lee and M. H. Cho, *Nanoscale,* 5, 9238 (2013).
35. M. Bielmann, P. Schwaller, P. Ruffieux, O. Groning, L. Schlapbach and P. Groning, *Phys Rev B*, 65, 235431 (2002).
36. J. F. Weaver and G. B. Hoflund, *J Phys Chem*, 98, 8519 (1994).
37. Y. Zheng, L. Zheng, Y. Zhan, X. Lin, Q. Zheng and K. Wei, *Inorg Chem*, 46, 6980 (2007).
38. S. Lany and A. Zunger, *Phys Rev B Condens Matter*, 78, 2351041 (2008).
39. M. R. Hoffmann, S. T. Martin, W. Choi and D. W. Bahnemannt, *Chem Rev*, 95, 69 (1995).